IEEE Access
Multidisciplinary | Rapid Review | Open Access Journal

Received 30 June 2022, accepted 31 July 2022, date of publication 5 August 2022, date of current version 11 August 2022.

Digital Object Identifier 10.1109/ACCESS.2022.3196851

RESEARCH ARTICLE

Improved Salp Swarm Optimization Algorithm for Damping Controller Design for Multimachine Power System

EHSAN AKBARI[1], MORTEZA MOLLAJAFARI[2], HAMZA MOHAMMED RIDHA AL-KHAFAJI[3], (Senior Member, IEEE), HUSSEIN ALKATTAN[4], MOSTAFA ABOTALEB[4], MAHDIYEH ESLAMI[5], (Member, IEEE), AND SIVAPRAKASAM PALANI[6]

[1]Department of Electrical Engineering, Mazandaran University of Science and Technology, Babol 4851878195, Iran
[2]School of Automotive Engineering, Iran University of Science and Technology, Tehran 16846-13114, Iran
[3]Biomedical Engineering Department, Al-Mustaqbal University College, Hillah, Babil 51001, Iraq
[4]Department of System Programming, South Ural State University, 454080 Chelyabinsk, Russia
[5]Department of Electrical Engineering, Kerman Branch, Islamic Azad University, Kerman 7635168111, Iran
[6]College of Electrical and Mechanical Engineering, Addis Ababa Science and Technology University, Addis Ababa 16417, Ethiopia

Corresponding authors: Mahdiyeh Eslami (mahdiyeh_eslami@yahoo.com) and Sivaprakasam Palani (shiva@aastu.edu.et)

ABSTRACT This paper proposes an improved salp swarm algorithm (ISSA) as an effective metaheuristic method for tackling global optimization issues and damping power system oscillations. In the suggested ISSA, new equations are introduced to update the location of the leader and followers. This modification improves the method's exploration possibilities while also preventing it from converging prematurely. Benchmark test functions are used to confirm the proposed algorithm's performance, and the results are compared to SSA and other effective optimization algorithms. According to the extensive comparisons, the enhanced ISSA algorithm has higher convergence accuracy and stability than the original SSA and other researched algorithms. Furthermore, the feasibility and efficiency of the proposed method were demonstrated by the simultaneous coordinated design of UPFC based damping controllers. For the two-area, four-machine system, the experimental findings are provided. Simulation experiments reveal that ISSA designed controllers outperform those created using other methods.

INDEX TERMS Damping, UPFC, salp swarm optimizer, stability.

I. INTRODUCTION

As a result of the integration of power systems, power system stability has become a major research topic. As a result, to improve stability, the power system has been improved with more complex control technology and better protective systems. Mechanical and electrical torque imbalances at the synchronous generator, which are generated by changes in power system topology or loads, create power system electromechanical oscillations, which can be divided into inter-area and local modes [1]. When low frequency oscillations are not adequately damped, they cause serious damage to the generator rotor shaft and power transfers. These oscillations have a substantial impact on a power supply's dependability and security. In order to address these unfavorable occurrences, power system stabilizers (PSSs) have long been employed to promote power system stability and raise system dampening of oscillation modes. These stabilizers dampen the generator rotor oscillations induced by the generator's speed, frequency, or power. However, because power networks are nonlinear and complicated, it is preferable to tackle any nonlinearity in the tuning problem with nonlinear models rather than linear approximations. Furthermore, the current study shows that the required damping level cannot be achieved if only one PSS is tuned. As a result, it is recommended that all PSS design processes be coordinated. According to literature reviews such as [1], PSSs regulators strength sometimes fail to provide appropriate damping torque for

The associate editor coordinating the review of this manuscript and approving it for publication was Amin Zehtabian.

inter-area modes. Unfortunately, there are some flaws in the dampening of inter-area oscillations, necessitating the use of other remedies. In recent years, power electronic-based FACTS controllers have been pushed as cost-effective solutions. FACTS devices have been used to solve a variety of power system control issues in the past [2]. In other words, they can improve power system stability and controllability by increasing power transmission capabilities. Therefore, power flow will be better managed, and voltages will be better kept within their rated limits, allowing for increased stability margins and a tendency toward the lines' thermal limitations. However, combining PSSs and FACTS devices in the same network has created a new difficulty for these regulators in terms of coordination. Indeed, it is critical to ensure that there is appropriate coordination between these devices so that their actions do not compromise the network's security.

The unified power flow controller (UPFC) is one of the best essential and complete FACTS devices, with the ability to regulate power flow in transmission lines via a series converter and input voltage via a shunt converter [3], [4]. Through its supplemental control, the UPFC can provide a substantial dampening impact on tie-line power oscillation when applied to interconnected power systems. As a result, a fixed parameter controller based on conventional control model is unlikely to be appropriate for UPFC based power oscillation damping control (POD). As a result, the development of a flexible controller is required.

For damping controller design, several methods have been presented, including root locus and sensitivity analysis, pole positioning, and robust control. These systems have significant limitations because the control law is based on a linearized machine model and the control bounds are tuned to specified nominal operating conditions. Additionally, controller parameters are inacceptable because system circumstances vary nonlinearly in the presence of substantial disturbances. Many classic approaches, such as linear programming, nonlinear programming, and quadratic programming, have been used to tackle the damping problem. Despite the algorithms' dependability, they all have flaws such as algorithmic complexity, unstable convergence, inability to handle nonlinear functions, and take in in local optima. The design of an optimum damping controller is a multifaceted optimization problem with several local minima.

These limitations are circumvented by meta-heuristic optimization approaches, which avoid linearizing the objective function by picking a collection of random solutions, which are then efficient about the greatest result in an iterative procedure till the procedure converges and the optimal result is took. New meta-heuristics optimization procedures created on theories for example evolutionary stimulated algorithms, human stimulated algorithms, and natural stimulated algorithms have been developed to overwhelm the problems of customary approaches, as meta-heuristics optimization techniques do not require a linear approximation of the nonlinear objective function, as traditional methods do. The techniques for solving the POD controller design challenge are shown in Fig. 1. As a result, substantial research has been done to apply various optimization strategies for the answer, such as the genetic algorithm (GA) [5], [6], particle swarm optimization (PSO) [4], [7]–[10], differential evolution (DE) [11], and gravitational search algorithm (GSA) [12], an important variety of similar algorithms have lately been proposed for coordinated design of power system controllers, including: ant colony optimization (ACO) [13], bee colony algorithm (BCA) [14], Genetic Algorithm (GA) [15], sine-cosine algorithm (SCA) [16], [17], grey wolf optimizer (GWO) [18], Cuckoo Search (CS) algorithm [19], Sperm Swarm Optimization (SSO) [20], Tabu Search (TS) [21], Simulated Annealing [22], Firefly Algorithm (FA) [23], [24], Multi-Verse Optimizer (MVO) [25] and Tunicate Swarm Algorithm (TSA) [26] have been successfully implemented to efficiently and effectively address basic and complicated problems. Natural evolution is the inspiration for the majority of population-based search strategies. Although the fact that metaheuristic algorithms can produce appropriate effects, no algorithm can outstrip others in resolving all optimization subjects. Consequently, several educations have been showed to growth the presentation and ability of the unique metaheuristic algorithms and adjust them to a definite request.

A new meta-heuristic algorithm called the Salp Swarm Algorithm (SSA) simulates salp fish swarming in deep waters [27]. Section 2 contains more information on the SSA algorithm's motivation and mathematical modelling. The SSA in its basic model, which can be extended or hybridized with another algorithm to produce better answers for future problems, similar to metaheuristic approaches [28], [29].

This paper presents an improved salp swarm optimization (ISSA) algorithm by proposing new updating equations for adjusting the position of the leader and followers. This modification improves the algorithm's performance and convergence speed significantly. A set of well-known standard benchmark functions from the literature is used to validate the effectiveness of the proposed approach. The new technique is also used to develop a UPFC based POD controller in this study. The numerical studies demonstration that the suggested algorithm congregates faster to a much more accurate final result. Moreover, the unique method's feasibility and effectiveness were demonstrated by the UPFC controllers' design is being coordinated at the same time. The results show that the ISSA designed controllers outperform those created using other methods in terms of oscillation damping and considerably improve dynamic stability. Furthermore, the results demonstrate that the new strategy outperforms other similar methods.

The following are the primary contributions of this work:

(1) An improved optimization approach, ISSA, is suggested for coordinated design of UPFC based damping controllers.

(2) The suggested technique includes two new equations for the leader's and followers' position updating procedures (ISSA). This modification broadens the algorithm's

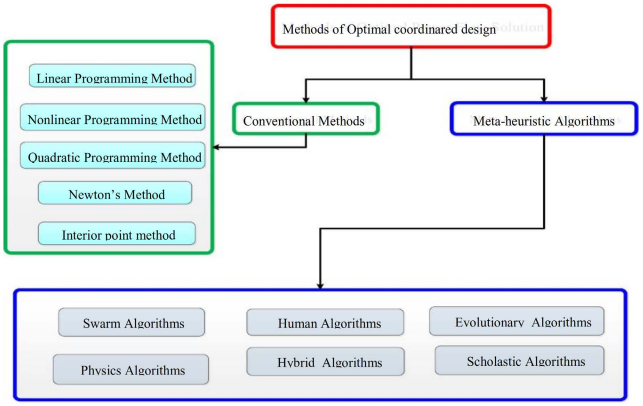

FIGURE 1. Methods of optimal coordinated problem.

exploration possibilities while also preventing it from converging prematurely.

(3) When compared to the original SSA and two algorithms for the damping of power system oscillation, ISSA outperforms them in terms of accuracy and stability.

The following is how the rest of the paper is structured: The proposed enhanced optimization approach is explained in Section 2. In Section 3 and 4, the problem is expressed as an optimization problem. Model verification is discussed in Section 5. The findings of the simulation are described in Section 6. Finally, the study's findings are described in Section 7.

II. SALP SWARM ALGORITHM

A salp is a type of marine organism in the Salpidae family.

It has a cylindrical structure with apertures at the ends, similar to jellyfish, which move and eat by pumping water through internal feeding filters in their gelatinous bodies. The salp swarm algorithm (SSA), a population-based optimization technique, was developed by Mirjalili *et al.* [27]. The salp chain can be used to calculate the SSA's behavior while hunting for optimal feeding sources (i.e., the target of this swarm is a food position in the search space called FP). To mathematically model salp chains, the sample into two groups: leaders and followers. The salp at the head of the chain is known as the leader, while the others are known as followers. The swarm is led by the leader of these salps, and the followers follow in his footsteps. The chain begins with a leader, who is followed by the followers to guide their movements.

Similar to other swarm-based algorithms, Salps' location is specified in a n–dimensional search space, where n is the number of variables in a given problem. As a result, the positions of all salps are recorded in a two-dimensional matrix known as X, as shown in Eq (1).

$$X_i = \begin{bmatrix} x_1^1 & x_2^1 & \cdots & x_d^1 \\ x_1^2 & x_2^2 & \cdots & x_d^2 \\ \vdots & \vdots & \cdots & \vdots \\ x_1^n & x_2^n & \cdots & x_d^n \end{bmatrix} \tag{1}$$

The fitness of each salp is then determined in order to determine which salp has the best fitness. It's also assumed that the swarm's target is a food position called FP in the search space.

The following equation can be used by the leader salp to change positions:

$$x_i^1 = \begin{cases} FP_i + c_1 \left((ub_i - lb_i) r_1 + lb_i \right) & r_2 \geq 0 \\ FP_i - c_1 \left((ub_i - lb_i) r_1 + lb_i \right) & r_2 < 0 \end{cases} \tag{2}$$

where x_i^1 denotes the first salp's position in the ith dimension and FP_i denotes the food position in the ith dimension. The lower and upper bounds of the ith dimension are represented by lb_i and ub_i, respectively, and the coefficient c_1 is calculated by Eq. (3). The random numbers r_1 and r_2 are between 0 and 1.

$$c_1 = 2e^{-\left(\frac{4t}{t_{max}}\right)^2} \tag{3}$$

where

t_{max}: The maximum number of iterations

t: The current iteration

It's worth noting that the c_1 coefficient is critical in SSA because it balances exploration and exploitation throughout the search. The following equations are used to change the position of the followers.

$$x_i^j = \frac{1}{2}\left(x_i^j + x_i^{j-1}\right) \tag{4}$$

where j ≥ 2.

In case some salps move outside of the search space, Eq. (6) shows how to bring salps back into the search space if they leave it.

$$x_i^j = \begin{cases} lb_i & if\ x_i^j \leq lb_i \\ ub_i & if\ x_i^j \geq ub_i \\ x_i^j & otherwise \end{cases} \tag{5}$$

The pseudocode of SSA is shown in Algorithm 1.

Algorithm 1 Salm Swarm Algoithm

Initialize the salp population $x_i (1 = 1, 2, \ldots, n)$ considering lb_i and ub_i
while $t \leq_{max}$
  Calculate the fitness of each search agent (salp)
  Put the best search agent as FP (Food position)
  Update c_1 by Eq. (3)
   for each salp (x_i)
    if $i == 1$
     Update the position of the leading salp by Eq. (2)
    else
     Update the position of the following salp
     by Eq. (4)
    end
   end
   Amend the salps based on the upper and lower bounds of variables
  Calculate the fitness of each search agent FP
  Update the food position
  $t = t + 1$
  end
return the food position FP and its best fitness

III. IMPROVED SALP SWARM ALGORITHM (ISSA)

Despite the SSA's ability to generate efficient results in comparison to other well-known algorithms, it is prone towards becoming stuck in a local optimum, making it unsuitable for very complex problems with multiple local optima.

As shown in Eq. 2, in the SSA, the leading salp modifies its location in respect to the position of the best salp in the entire population (i.e., food situation). This means that at each iteration pass, the SSA algorithm adjusts the location of the leader salp around a single point, and additional salps (followers) follow the leader. Therefore, when the algorithm converges, it loses its exploration ability and becomes frozen at local minimum locations. According to these situations, an improved version of the SSA (ISSA) is presented to fix the aforementioned problem while simultaneously boosting the search capabilities and flexibility of the algorithm. In the proposed ISSA, to increase the algorithm's performance and exploring capabilities, the leader salp updates its location not only based on the placement of the food source but also its previous position. To update the position of the leader salp, use the following equation:

$$x_i^1 = \begin{cases} x_i^j + c_1 \times \left(FP_i - x_i^j\right) & r_2 \geq 0.5 \\ x_i^j - c_1 \times \left(FP_i - x_i^j\right) & r_2 < 0.5 \end{cases} \tag{6}$$

In Eq. (6) c_1 is a time-varying parameters obtained by Eq. (3) and r_2 is a random number between 0 and 1. This strategy permits exploration while also enabling the SSA algorithm to perform a more successful global search throughout the entire search space. To enhance the query performance of the suggested ISSA, the followers will change their position through using the following equation:

$$x_i^j = c_1 \times rand\left(x_i^j + x_i^{j-1}\right) \tag{7}$$

In Eq. (7), a random time-varying factor is considered instead of the constant value of 0.5 presented in the standard algorithm. This factor increases the global search ability of the algorithm in early iterations and local search capability in late iterations. In addition, in the recommended ISSA, at each algorithm's generation, the salp with the greatest fitness value will be changed by a randomly generated salp. Figure 2 depicts the proposed ISSA algorithm's flowchart.

A. COMPARATIVE TIME COMPLEXITY ANALYSIS

Most algorithms' time complexity analysis includes three component analyses. Similarly, ISSA's temporal complexity analysis necessitates examination of these three components:

1. The time complexity of population initialization is often bounded by $\Phi\ (n \times d)$, where n signifies population size and d denotes problem dimensions/design factors.

2. Initial fitness evaluation time complexity is often bounded $\Phi\ (n \times C_{0bj})$, where C_{obj} denotes the cost of the objective function.

3. The time complexity of the key loop is often bounded by $(t_{max} \times (n \times d + n \times C_{0bj}))$, where M t_{max} is the maximum number of iterations.

As a result, the overall time complexity of the ISSA method is $(t_{max} \times (n \times d + \times C_{0bj}))$.

IV. PROBLEM FORMULATION

A. DYNAMIC MODEL OF THE UPFC

The UPFC is a multipurpose FACTS controller with a broad variety of control capabilities for power system presentation enhancement [30]. Figure 3 depicts a power system with a UPFC. $m_{B,}\delta_E, \delta_{B,}$ *and* m_E are the four input control signals to the UPFC. These characteristics are used as UPFC control inputs in series lines without an external voltage source to enable synchronized power correction [4]. In order to explore the influence of the UPFC on improving the power system's small-signal stability, a dynamic model of the UPFC is necessary. UPFC can be modelled as follows [30], [31]:

$$\begin{aligned} \frac{dv_{dc}}{dt} &= \frac{3m_E}{4C_{dc}} \begin{bmatrix} \cos\delta_E & \sin\delta_E \end{bmatrix} \begin{bmatrix} i_{Ed} \\ i_{Eq} \end{bmatrix} \\ &\quad + \frac{3m_B}{4C_{dc}} \begin{bmatrix} \cos\delta_B & \sin\delta_B \end{bmatrix} \begin{bmatrix} i_{Bd} \\ i_{Bq} \end{bmatrix} \end{aligned} \tag{8}$$

$$\begin{bmatrix} v_{Etd} \\ v_{Eiq} \end{bmatrix} = \begin{bmatrix} 0 & -x_E \\ x_E & 0 \end{bmatrix} \begin{bmatrix} i_{Ed} \\ i_{Eq} \end{bmatrix} + \begin{bmatrix} \frac{m_E \cos\delta_E v_{dc}}{2} \\ \frac{m_E \sin\delta_E v_{dc}}{2} \end{bmatrix}$$

$$\begin{bmatrix} v_{Btd} \\ v_{Biq} \end{bmatrix} = \begin{bmatrix} 0 & -x_B \\ x_B & 0 \end{bmatrix} \begin{bmatrix} i_{Bd} \\ i_{Bg} \end{bmatrix} + \begin{bmatrix} \frac{m_B \cos\delta_B v_{dc}}{2} \\ \frac{m_B \sin\delta_B v_{dc}}{2} \end{bmatrix} \tag{9}$$

where

m_E: Excitation amplitude modulation ratio.

δ_E: Excitation phase angle.

δ_B: Boosting phase angle.

m_B: Boosting amplitude modulation ratio.

Excitation voltage, boosting voltage, excitation current, and boosting current are represented by v_{Et}, v_{Bt}, i_E, and i_B, respectively, and DC link capacitance and voltage are represented by C_{dc} and v_{dc}, respectively. In addition, the ET reactance is x_E, and the BT reactance is x_B.

B. UPFC- BASED POD

To increase damping of system oscillations, the controller is meant to provide an electrical torque in-phase with the speed variation utilizing the phase correction approach. To produce the damping torque, the 4 control bounds of the UPFC can be changed as follows:

Active power regulator:

$$\delta_B = \left(\frac{1}{1 + T_{\delta B}s}\right)\left(K_{pp} + \frac{K_{pi}}{s}\right)\left(P_{Ref} - P\right) \tag{10}$$

Reactive power regulator:

$$m_B = \left(\frac{1}{1 + T_{mB}s}\right)\left(K_{qp} + \frac{K_{qi}}{s}\right)\left(Q_{Ref} - Q\right) \tag{11}$$

AC voltage regulator:

$$m_E = \left(\frac{1}{1 + T_{mE}S}\right)\left(K_{vp} + \frac{K_{vi}}{s}\right)\left(V_{Ref} - V\right) \tag{12}$$

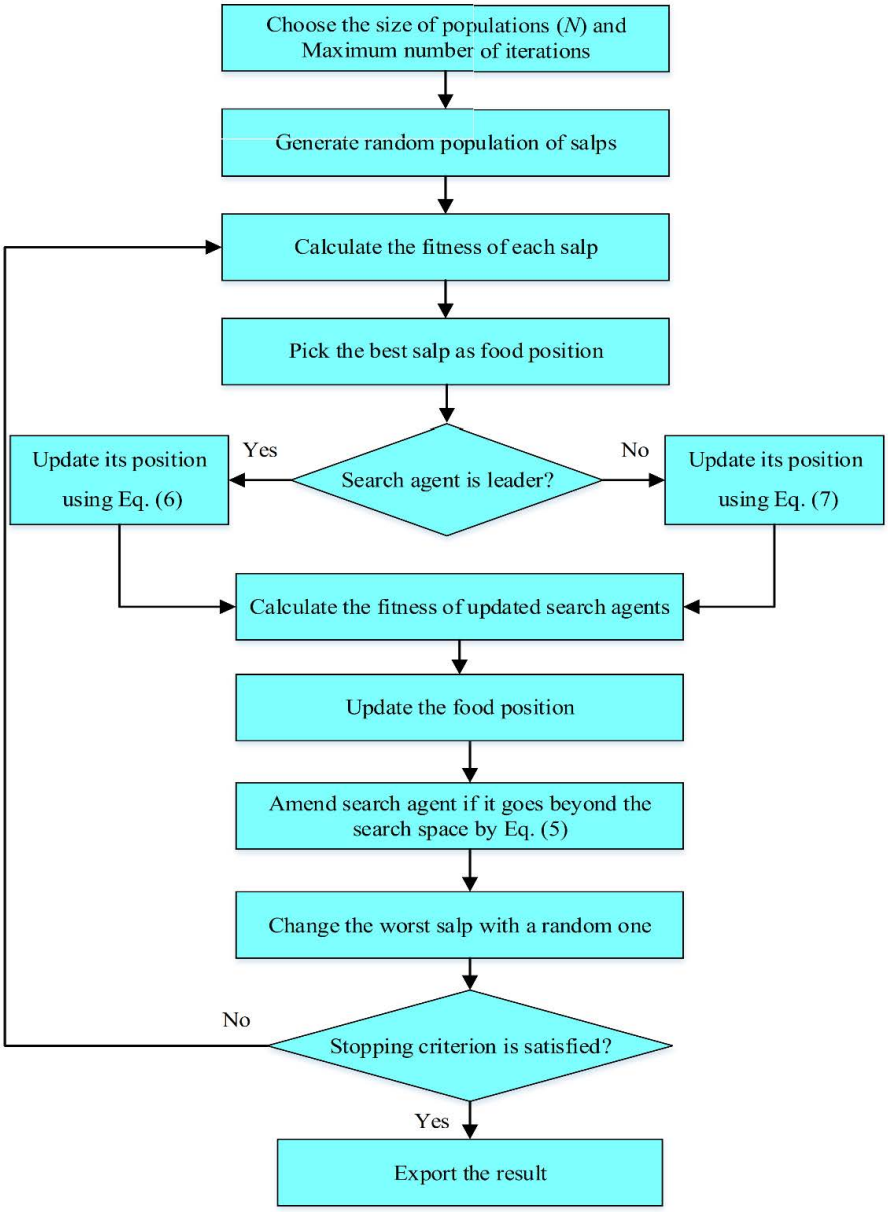

FIGURE 2. Flowchart of the ISSA.

DC voltage regulator:

$$\delta_E = \left(\frac{1}{1+T_{\delta E}s}\right)\left(K_{dcp}+\frac{K_{dci}}{s}\right)\left(v_{DCref}-V_{DC}\right) \quad (13)$$

The UPFC controller's construction is given in Fig. 4, where u could be m_E, m_B, δ_E, and δ_B. A dc voltage regulator must be included to keep the electricity flowing between the shunt and series converters. The phase angle of the ET voltage δ_E is modulated to regulate the dc voltage. Additional control act is utilized to excitation of the generator in the form of a PSS or UPFC as a POD controller to ease the low frequency oscillation problem.

To provide the required damping torque, the four primary control limits of the UPFC can be modified, as shown in Fig. 5. Two controllers are coupled to the UPFC to damp the oscillation modes that are not effectively damped oscillations. The controllers can be added to the UPFC's standard control capabilities. The first controller can be connected to the m_E function to dampen inter-area oscillations, while the second controller can be connected to the δ_E function to dampen local oscillations. Figure 5 depicts the δ_E damping controller to be examined. A PI controller controls the DC voltage regulator. The m_E damping controller is nearly identical to the δ_E damping controller, with the exception that AC voltage regulation is handled by a PI controller.

Based on the linearized typical of the power system, two controllers overlaid on the functions of the UPFC's AC and DC voltage controls were developed in collaboration.

The construction of the POD controller is identical to that of the PSS. To increase the damping of power system

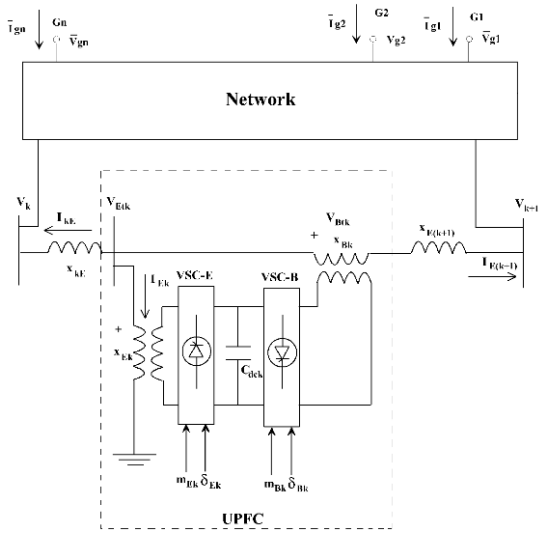

FIGURE 3. Power system with UPFC.

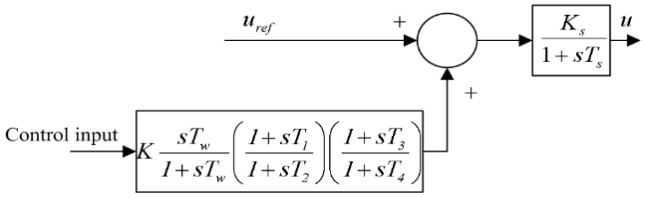

FIGURE 4. UPFC controller.

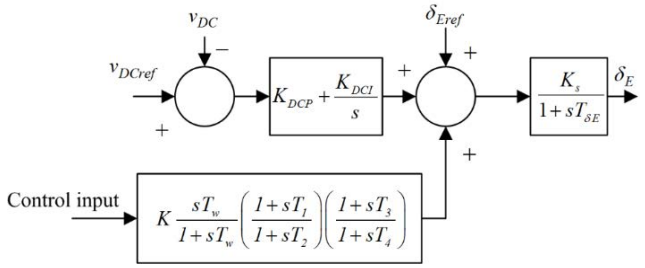

FIGURE 5. POD with damping controller and dc voltage regulator.

oscillations, the controller produces an electrical torque in step with the speed deviation. The electromechanical oscillation modes should have a washout time *Tw* of 1–20 seconds. The time constant ($T\omega$) in this study is set to 10 seconds. The damping controller parameters (K, $T1$ to $T4$) are calculated using the ISSA technique.

C. LINEARIZED MODEL

Through linearizing the non-linear classical about an operational point of the power system, a linearized model with controllers can be produced as follows:

$$\begin{aligned}
\Delta\dot{\delta} &= \omega_0\Delta\omega \\
\Delta\dot{\omega} &= \mathbf{M}^{-1}\left(-\Delta\mathbf{T_E} - \mathbf{D}\Delta\omega\right) \\
\Delta\dot{\mathbf{E}}'_{\mathbf{q}} &= \mathbf{T}'^{-1}_{\mathbf{D0}}\left[-\Delta\mathbf{E}'_{\mathbf{q}} - \left(\mathbf{X_D} - \mathbf{X}'_{\mathbf{D}}\right)\Delta\mathbf{I_D} + \Delta\mathbf{E_{FD}}\right] \\
\Delta\dot{\mathbf{E}}_{\mathbf{FD}} &= \left(-\Delta\mathbf{E_{FD}} + \mathbf{K_A}\left(\Delta\mathbf{V_{RcI}} - \Delta\mathbf{V_T} + \Delta\mathbf{U_{PSS}}\right)\right)\mathbf{T}_{\mathbf{A}}^{-1} \\
\Delta\mathbf{T_E} &= \Delta\mathbf{I_Q}\dot{\mathbf{E}}'_{\mathbf{q0}} + \mathbf{I_{Q0}}\Delta\dot{\mathbf{E}}'_{\mathbf{q}} + \Delta\mathbf{I_Q}\left(\mathbf{X_Q} - \mathbf{X}'_{\mathbf{D}}\right)\mathbf{I_{D0}} \\
&\quad + \Delta\mathbf{I_D}\left(\mathbf{X_Q} - \mathbf{X}'_{\mathbf{D}}\right)\mathbf{I_{Q0}} \\
\Delta\mathbf{V_{TD}} &= \mathbf{X_Q}\Delta\mathbf{I_Q}, \quad \Delta\mathbf{V_{TQ}} = \Delta\dot{\mathbf{E}}'_{\mathbf{q}} - \mathbf{X}'_{\mathbf{v}}\Delta\mathbf{I_D}
\end{aligned} \tag{14}$$

where

$$\begin{aligned}
\Delta\mathbf{T} &= \mathbf{K}_1\Delta\delta + K_2\Delta\mathbf{E}'_q + \mathbf{K_{pd}}\Delta v_{DC} + \mathbf{K_{pe}}\Delta m_E \\
&\quad + \mathbf{K_{pde}}\Delta\delta_E + \mathbf{K_{pb}}\Delta m_B + \mathbf{K_{pdb}}\Delta\delta_B \\
\Delta\mathbf{E_q} &= \mathbf{K}_4\Delta\delta + \mathbf{K}_3\Delta\mathbf{E}'_q + \mathbf{K_{qd}}\Delta v_{DC} + \mathbf{K_{qc}}\Delta m_E \\
&\quad + \mathbf{K_{qde}}\Delta\delta_E + \mathbf{K_{qb}}\Delta m_B + \mathbf{K_{qdb}}\Delta\delta_B \\
\Delta\mathbf{V_t} &= \mathbf{K}_5\Delta\delta + \mathbf{K}_6\Delta E'_q + \mathbf{K_{vd}}\Delta v_{DC} \\
&\quad + \mathbf{K_{ve}}\Delta m_E + \mathbf{K_{vde}}\Delta\delta_E + \mathbf{K_{vb}}\Delta m_B + \mathbf{K_{vdb}}\Delta\delta_B \\
\Delta\dot{v}_{DC} &= K_7\Delta\delta + K_8\Delta E'_q - K_g\Delta v_{DC} + K_{ce}\Delta m_E \\
&\quad + K_{c\delta\varepsilon}\Delta\delta_E + K_{cb}\Delta m_B + K_{cbb}\Delta\delta_B
\end{aligned} \tag{15}$$

In state-space representation, the equation can be organized as follows:

$$\Delta\dot{X} = A\Delta X + B\Delta U \tag{16}$$

The state and control vectors, respectively, are ΔX and ΔU. The matrices A and B have the following structure as (17), shown at the bottom of the next page.

D. OPTIMUM DESIGN

The controller's design aim is to locate the eigenvalues of matrix A in the complex plane's left side. To improve the damping of the modes, a multi-objective function based on the damping ratio and damping factor is examined, and the objective function is as follows:

$$\begin{aligned}
J &= \sum\nolimits_{\sigma_0>\sigma_0}(\sigma_0 - \sigma_i)^2 + \alpha\sum\nolimits_{\zeta_i>\zeta_0}(\zeta_0 - \zeta_i)^2, \\
f(x) &= min\, J
\end{aligned} \tag{18}$$

The predicted damping factor and damping ratio have constant values of σ_0 and ζ_0, respectively. By minimizing the $f(x)$, the system modes are changed to a D-shape area.

The design challenge can be described as the following constrained optimization problem, with the constraints being the POD controller parameter boundaries.

$$K_{min} \le K \le K_{max}, \quad T_{imin} \le T_i \le T_{imax} \quad i = 1, \ldots, 4 \tag{19}$$

where

K: Gain of controller

$T_1 - T_4$: Time constant (s)

The ISSA is used in the suggested approach to resolve this problem and find the best set of controller parameters. When applying the penalty technique to optimize the controller's settings, the inequality restrictions stated in Eq. (19) should be taken into account. The optimized parameters' typical ranges are 0.01–100 for K and 0.01–2 for T.

TABLE 1. Explanation of unimodal functions.

Function	*Name*	*Range*	f_{min}	*dim*
$F_1(X) = \sum_{i-1}^{n} x_i^2$	Sphere function	$[-100, 100]^n$	0	30
$F_2(X) = \sum_{i=1}^{n} \lvert x_i \rvert + \prod_{i=1}^{n} \lvert x_i \rvert$	Schwefel's problem 2.22	$[-10, 10]^n$	0	30
$F_3(X) = \sum_{i=1}^{n} \left(\sum_{j=1}^{i} x_j \right)^2$	Schwefel's problem 1.2	$[-100, 100]^n$	0	30
$F_4(X) = \max_i \{ \lvert x_i \rvert, 1 \le i \le n \}$	Schwefel's problem 2.21	$[-100, 100]^n$	0	30
$F_5(X) = \sum_{i=1}^{n-1} \left[100 \left(x_{i+1} - x_i^2 \right)^2 + (x_i - 1)^2 \right]$	Generalized Rosenbrock's function	$[-30, 30]^n$	0	30
$F_6(X) = \sum_{i=1}^{n} ([x_i + 0.5])^2$	Step function	$[-100, 100]^n$	0	30
$F_7(X) = \sum_{i=1}^{n} i x_i^4 + random[0, 1)$	Quartic function with noise	$[-1.28, 1.28]^n$	0	30

V. MODEL VERIFICATION

A set of numerical reference test functions has been used in this section to compare and confirm the achievement and effectiveness of the proposed ISSA.

In the empirical evidence literature, these functions are commonly used to determine the performance of optimizers [26], [32]. The mathematical model and characteristics of these test functions are shown in Tables 1-2. This standard set is divided into two categories: unimodal functions with a single global best for testing algorithm convergence pace and enslavement ability, and multi - modal functions with multiple local minimums and a global ideal for testing an algorithm's local optima avoidance and exploratory capacity. MATLAB R2020b was used to create the suggested algorithms. All of these functions, should be minimized. Furthermore, all functions have a dimension of 30. Three-dimensional drawings of these benchmark functions are illustrated in Figures 6 and 7. The proposed ISSA is compared to the original SSA as well as some well-known optimization methods such as Particle Swarm Optimization (PSO) proposed by [33], Firefly Algorithm (FA) introduced by [34], Multi-Verse Optimizer (MVO) developed by [25] and Tunicate Swarm Algorithm (TSA) introduced by [26].

According to the literature [35] and for a fair comparison of the selected techniques, the size of solutions (N) and maximum iteration number (t_{max}) for all algorithms are set to 30 and 1000, respectively.

Because the results of a single run of metaheuristic methods are stochastic, they may be incorrect. Accordingly, statistical analysis should be achieved in order to afford a reasonable contrast and evaluate the algorithms' efficacy. To address this issue, 30 times runs for the mentioned methods are performed, with the results presented in Tables 3-4. Tables 3 and 4 demonstrate that, for all functions, ISSA could provide superior solutions in terms of mean value of the objective functions than conventional SSA and other methods. The results also show that the mean and standard deviation of the ISSA algorithm are significantly lower than those of the other strategies, representative that the algorithm is stable. ISSA outperforms both the standard method and alternative optimization approaches, according to the findings.

$$\begin{bmatrix} \Delta\dot{\delta} \\ \Delta\omega \\ \Delta\dot{\mathbf{E}}'_{\mathbf{q}} \\ \Delta\mathbf{E}_{\mathbf{fd}} \\ \Delta v_{DC} \end{bmatrix} = \begin{bmatrix} 0 & \omega_0\mathbf{I} & 0 & 0 & 0 \\ -\mathbf{M}^{-1}\mathbf{K}_1 & -\mathbf{M}^{-1}\mathbf{D} & -\mathbf{M}^{-1}\mathbf{K}_2 & 0 & -\mathbf{M}^{-1}\mathbf{K}_{\mathbf{pd}} \\ -\mathbf{T}_{\mathbf{do}}^{+-1}\mathbf{K}_4 & 0 & -\mathbf{T}_{\mathbf{do}}^{\prime-1}\mathbf{K}_3 & \mathbf{T}_{\mathbf{do}}^{\prime-1} & -\mathbf{T}_{\mathbf{do}}^{\prime-1}\mathbf{K}_{\mathbf{qd}} \\ -\mathbf{T}_{\mathbf{A}}^{-1}\mathbf{K}_{\mathbf{A}}\mathbf{K}_5 & 0 & -\mathbf{T}_{\mathbf{A}}^{-1}\mathbf{K}_{\mathbf{A}}\mathbf{K}_6 & \mathbf{T}_{\mathbf{A}}^{-1} & -\mathbf{T}_{\mathbf{A}}^{-1}\mathbf{K}_{\mathbf{A}}\mathbf{K}_{\mathbf{vd}} \\ K_7 & 0 & K_8 & 0 & -K_9 \end{bmatrix} \begin{bmatrix} \Delta\delta \\ \Delta\omega \\ \Delta\mathbf{E}'_{\mathbf{q}} \\ \Delta\mathbf{E}_{\mathbf{fd}} \\ \Delta v_{DC} \end{bmatrix} + \begin{bmatrix} 0 & 0 & 0 & 0 \\ -\mathbf{M}^{-1}\mathbf{K}_{\mathbf{pe}} & -\mathbf{M}^{-1}\mathbf{K}_{\mathbf{pde}} & -\mathbf{M}^{-1}\mathbf{K}_{\mathbf{pb}} & -\mathbf{M}^{-1}\mathbf{K}_{\mathbf{pdb}} \\ -\mathbf{T}_{\mathbf{do}}^{\prime-1}\mathbf{K}_{\mathbf{qe}} & -\mathbf{T}_{\mathbf{do}}^{+1}\mathbf{K}_{\mathbf{qde}} & -\mathbf{T}_{\mathbf{do}}^{\prime-1}\mathbf{K}_{\mathbf{qb}} & -\mathbf{T}_{\mathbf{do}}^{-1}\mathbf{K}_{\mathbf{qdb}} \\ -\mathbf{T}_{\mathbf{A}}^{-1}\mathbf{K}_{\mathbf{A}}\mathbf{K}_{\mathbf{ve}} & -\mathbf{T}_{\mathbf{A}}^{-1}\mathbf{K}_{\mathbf{A}}\mathbf{K}_{\mathbf{vde}} & -\mathbf{T}_{\mathbf{A}}^{-1}\mathbf{K}_{\mathbf{A}}\mathbf{K}_{\mathbf{vb}} & -\mathbf{T}_{\mathbf{A}}^{-1}\mathbf{K}_{\mathbf{A}}\mathbf{K}_{\mathbf{vdb}} \\ K_{ce} & K_{c\delta e} & K_{cb} & K_{c\delta b} \end{bmatrix} \begin{bmatrix} \Delta m_E \\ \Delta\delta_E \\ \Delta m_B \\ \Delta\delta_B \end{bmatrix} \tag{17}$$

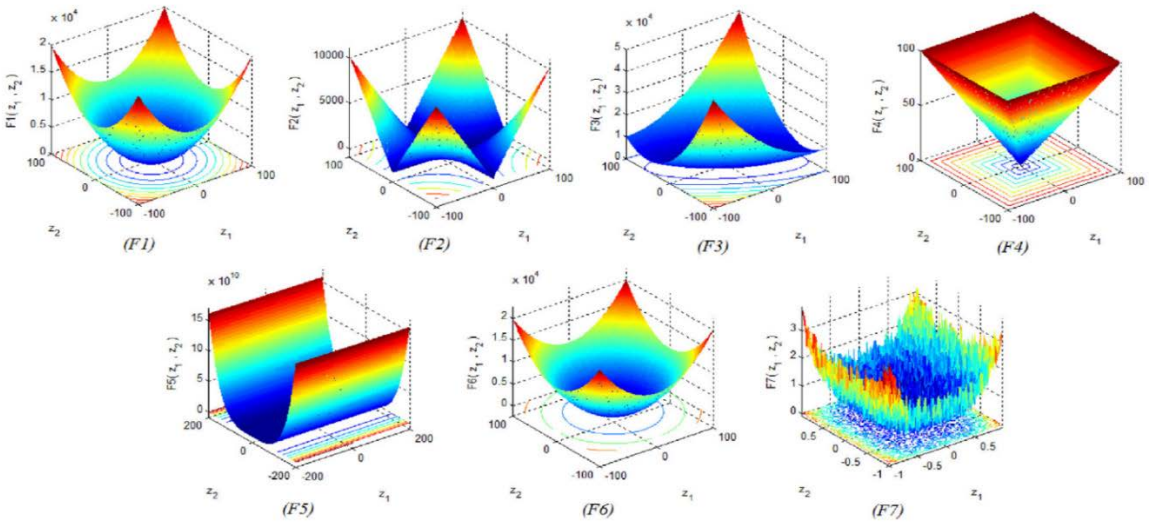

FIGURE 6. 3-D types of unimodal functions.

TABLE 2. Explanation of multimodal functions.

Function	*Name*	*Range*	f_{min}	*dim*
$F_8(X) = \sum_{i=1}^{n} -x_i \sin(\sqrt{\lvert x_i \rvert})$	Generalized Schwefel's problem 2.26	$[-500, 500]^n$	428.9829 $\times n$	30
$F_9(X) = \sum_{i=1}^{n} [x_i^2 - 10\cos(2\pi x_i) + 10]$	Generalized Rastrigin's function	$[-5.12, 5.12]^n$	0	30
$F_{10}(X) = -20\exp\left(-0.2\sqrt{\frac{1}{n}\sum_{i=1}^{n} x_i^2}\right) - exp\left(\frac{1}{n}\sum_{i-1}^{n}\cos(2\pi x_i)\right) + 20 + e$	Ackley's function	$[-32, 32]^n$	0	30
$F_{11}(X) = \frac{1}{4000}\sum_{i=1}^{n} x_i^2 - \prod_{i=1}^{n}\cos\left(\frac{x_i}{\sqrt{i}}\right) + 1$	Ackley's function	$[-600, 600]^n$	0	30
$F_{12}(X) = \frac{\pi}{n}\left\{10\sin(\pi y_1) + \sum_{i=1}^{n-1}(y_i - 1)^2[1 + 10\sin^2(\pi y_{i+1})] + (y_n - 1)^2\right\} + \sum_{i=1}^{n} u(x_i, 10, 100, 4)$, $y_i = 1 + \frac{x_{i+4}}{4}$, $u(x_i, a, k, m) = \begin{cases} k(x_i - a)^m & x_i > a \\ 0 & a < x_i < a \\ k(-x_i - a)^m & x_i < -a \end{cases}$	Generalized penalized function	$[-50, 50]^n$	0	30
$F_{13}(X) = 0.1\left\{\sin^2(3\pi x_1) + \sum_{i=1}^{n}(x_i - 1)^2[1 + \sin^2(3\pi x_i + 1)] + (x_n - 1)^2[1 + \sin^2(2\pi x_n)]\right\} + \sum_{i=1}^{n} u(x_i, 5, 100, 4)$	Generalized penalized function	$[-50, 50]^n$	0	30

VI. MODEL APPLICATION

The effectiveness of the suggested approach were confirmed in the preceding section by taking into account a number of benchmark concerns. The applicability and efficacy of the suggested technique for designing controller parameters are examined in this section. Figure 8 depicts the two-area–four-machine setup that was used to prove the damping controller design. This system, which was first reported in [36], is used as a reference for inter-area oscillation study. For machines 2 and 3, two PSSs should be developed simultaneously [37]. The system data and small-signal stability definition are taken from [38]. The basic oscillations found in linked power systems are depicted in this simplified model. A UPFC is constructed between buses 7 and 10, with four PI controllers performing the active and reactive power control, as well as voltage regulation, are the primary functions.

To address this problem and discover the best set of controller bounds, the ISSA is used in the presented approach. This approach has a good stabilizer and can handle a varied variety of operational scenarios. It's worth noting that the ISSA algorithm should be run numerous times before the best set of controller parameters is chosen. The final standards of the optimized parameters utilizing the objective function, J,

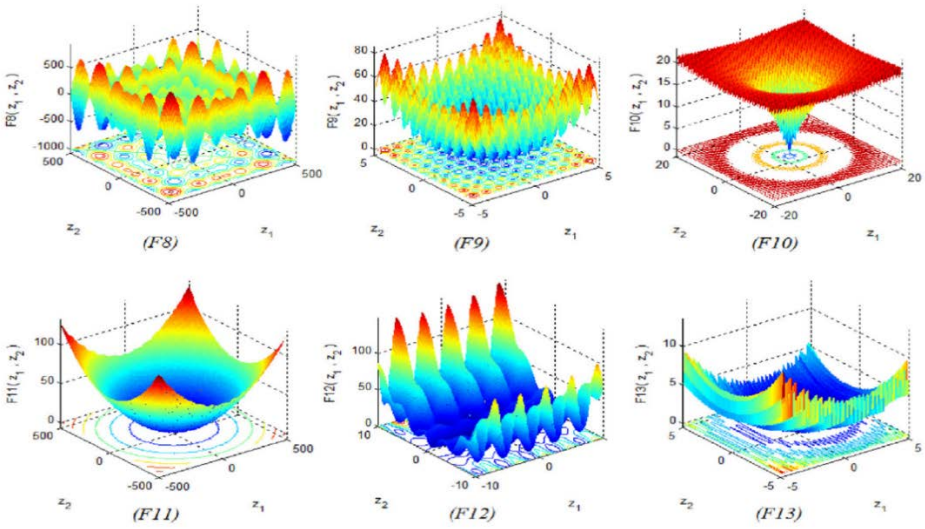

FIGURE 7. 3-D types of multimodal functions.

TABLE 3. Comparison of approaches in resolving unimodal functions.

F	Index	ISSA	SSA	PSO	FA	MVO	TSA
F_1	Mean	**0.00**	3.29E-07	4.98E–09	7.11E–03	2.81E–01	8.31E–56
	Std.	**0.00**	5.92E–07	1.40E–08	3.21E–03	1.11E–01	1.02E–58
F_2	Mean	**0.00**	1.9111	7.29E–04	4.34E–01	3.96E–01	8.36E–35
	Std.	**0.00**	1.6142	1.84E–03	1.84E–01	1.41E–01	9.86E–35
F_3	Mean	**0.00**	1.50E+03	1.40E+01	1.66E+03	4.31E+01	1.51E–14
	Std.	**0.00**	707.05	7.13E+00	6.72E+02	8.97E+00	6.55E–14
F_4	Mean	**0.00**	2.44E–05	6.00E–01	1.11E–01	8.80E–01	1.95E–05
	Std.	**0.00**	1.89E–05	1.72E–01	4.75E–02	2.50E–01	4.49E–04
F_5	Mean	**4.33E–01**	136.56	4.93E+01	7.97E+01	1.18E+02	28.4E+00
	Std.	**7.64E–01**	154.00	3.89E+01	7.39E+01	1.43E+02	0.842
F_6	Mean	**3.84E–07**	5.72E–07	6.92E–02	6.94E–03	2.02E–02	3.67E+00
	Std.	**2.12E–07**	2.44E–07	2.87E–02	3.61E–03	7.43E–03	0.3353
F_7	Mean	**4.66E–06**	8.82E–05	8.94E–02	6.62E–02	5.24E–02	0.0018
	Std.	**3.42E–06**	6.94E–05	0.0206	4.23E–02	1.37E–02	4.62E–04

TABLE 4. Comparison of approaches in resolving multimodal functions.

F	Index	ZISSA	SSA	PSO	FA	MVO	TSA
F_8	Mean	**–1.21E+04**	–7.46 E+03	–6.01E+03	–5.85E+03	–6.92E+03	–7.89E+03
	Std.	**6.76E+02**	634.67	1.30E+03	1.61E+03	9.19E+02	599.26
F_9	Mean	**0.00**	55.45E+00	4.72E+01	1.51E+01	1.01E+02	151.45
	Std.	**0.00**	18.27E+00	1.03E+01	1.25E+01	1.89E+01	35.87
F_{10}	Mean	**8.88E–16**	2.84E+00	3.86E–02	4.58E–02	1.15E+00	2.409
	Std.	**0.00**	6.58 E–01	2.11E–01	1.20E–02	7.87E–01	1.392
F_{11}	Mean	**0.00**	2.29 E–01	5.50E–03	4.23E–03	5.74E–01	0.0077
	Std.	**0.00**	1.29 E–01	7.39E–03	1.29E–03	1.12E–01	0.0057
F_{12}	Mean	**4.49E–04**	6.82E+00	1.05E–02	3.13E–04	1.27E+00	6.373
	Std.	**9.41E–04**	2.72E+00	2.06E–02	1.76E–04	1.02E+00	3.458
F_{13}	Mean	**2.86E–03**	21.31E+00	4.03E–01	2.08E–03	6.60E–02	2,897
	Std.	**3.65E–03**	16.99E+00	5.39E–01	9.62E–04	4.33E–02	0.643

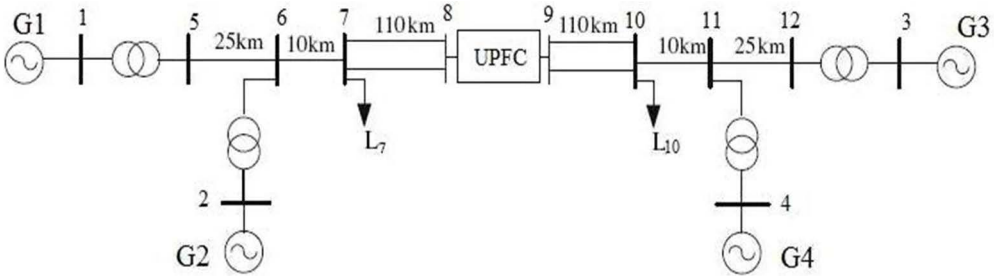

FIGURE 8. Test system with UPFC.

TABLE 5. Result of coordinated design by three methods.

controller Parameters	TSA based m_E	TSA based δ_E	SSA based m_E	SSA based δ_E	ISSA based m_E	ISSA based δ_E
T_1	0.54	0.71	0.47	0.26	0.31	0.37
T_2	0.04	0.04	0.38	0.09	0.05	0.043
T_3	0.64	0.09	0.14	0.28	0.15	0.45
T_4	0.21	0.01	0.03	0.26	0.06	0.05
K	25.76	49.56	64.76	39.65	27.25	25.36

TABLE 6. Oscillation modes with UPFC.

	Without any controllers	by TSA	by SSA	by ISSA
Local modes	-0.552±j7.32	-0.92±j5.87	-1.01± j5.41	-1.33±j5.445
	-0.531±j7.38	-0.1±j5.76	-1.03± j5.45	-1.51±j5.363
Inter-area mode	**0.044**±j4.03	-0.42±j3.89	-0.65±j3.67	-0.93±j3.283

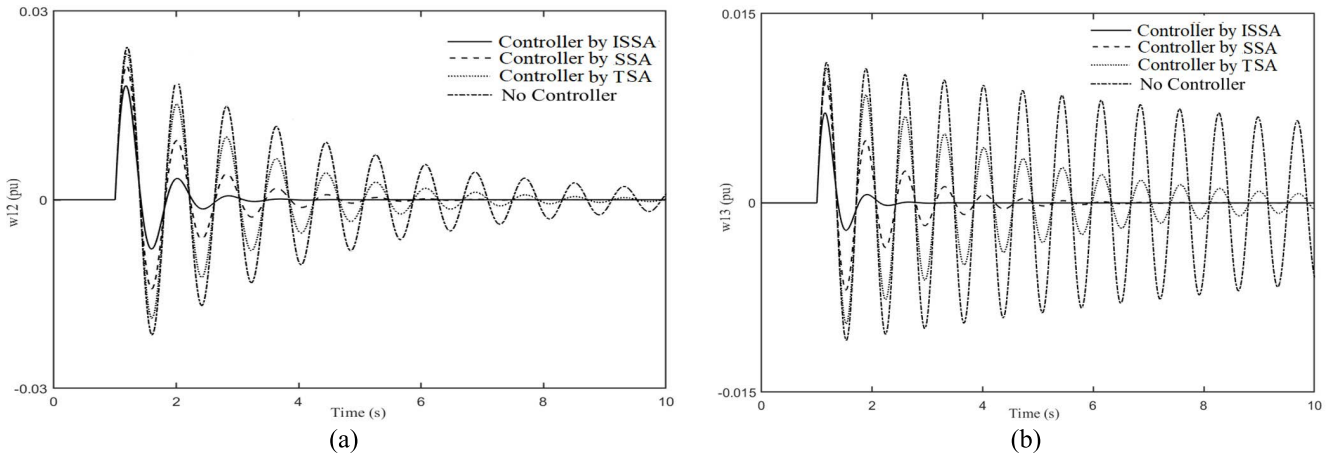

FIGURE 9. Speed deviation reply case I: (a) w_{12}; (b) w_{13}.

are shown in Table 5. The parameters acquired by the algorithms are sent to the research system.

The study system receives the parameters obtained by the algorithms. Table 6 shows the primary eigenvalues found for all operating situations after applying various optimization strategies to the system. Some of the modes are weakly damped in the system without a stabilizer, and the system is unstable under certain operating conditions. The proposed controllers significantly improve system stability. All modes are well damped after the controllers have been adjusted and coordinated. The ISSA, unlike the SSA and TSA, can relocate the worst eigenvalue to the D-shape sector. This feature increases the damping characteristic of the mode and considerably improves system stability.

It demonstrates that using the proposed strategy to improve global searching capability and performance stability is a viable option. For various fault disturbances, time-domain simulation is utilized to evaluate the efficiency and resilience of the suggested controllers. The response of the network to several disturbances is provided using generator G3 as the reference and the pre-disturbance operating condition in per units as $P_1 = 0.4444$, $Q_1 = 0.2056$, $P_2 = 0.6667$,

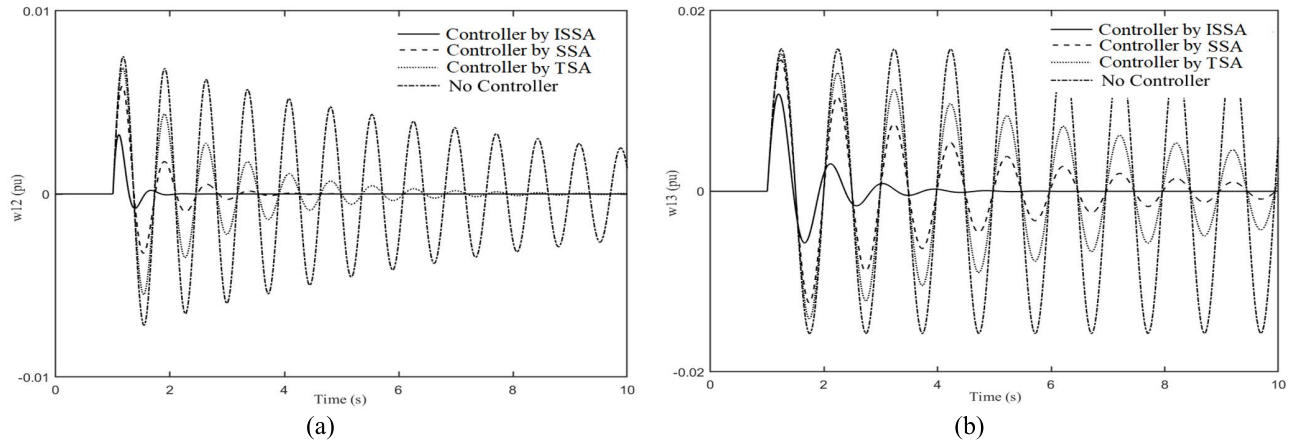

FIGURE 10. Speed deviation reply case II: (a) w_{12}; (b) w_{13}.

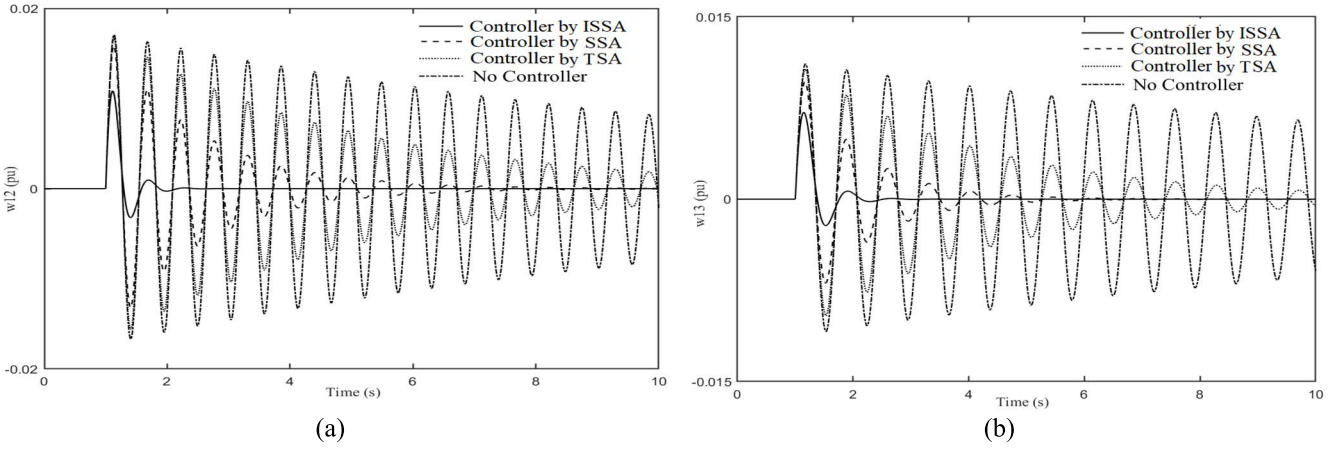

FIGURE 11. Speed deviation reply case III: (a) w_{12}; (b) w_{13}.

$Q_2 = 0.2611$, $P_3 = 1.5767$, $Q_3 = 0.2186$, $P_4 = 0.3333$ and $Q_4 = 0.2244$. The following case studies are used to evaluate the proposed controller's performance.

Case 1: A three-phase fault with a duration of 100 ms is simulated in the center of a line linking buses 7 and 8. The local and inter-area modes of oscillations are depicted in Figure 9. In comparison to the other optimization strategies, ISSA performs exceptionally well.

Case 2: A 100-ms three-phase failure is simulated in the central of one of the transmission lines linking buses 9 and 10, under the identical operative conditions as Case 1. Figure 10 depict the inter-area and local modes of oscillations. The proposed approach is found to be effective in dampening oscillations in both the inter-area and local modes.

Case 3: To evaluate the success of the recommended technique in a multi-machine situation, the power network's operational circumstances are changed to $P_1 = 0.5556$, $Q_1 = 0.2056$, $P_2 = 0.5556$, $Q_2 = 0.2611$, $P_3 = 1.3739$, $Q_3 = 0.1502$, $P_4 = 0.5556$, and $Q_4 = 0.2244$. Case 2's three-phase fault is initiated for 100 milliseconds. The oscillation modes for the transient disturbance are shown in Figure 11. The proposed controllers' very effective performance is demonstrated by these responses. When the results of the presented approach, SSA, and TSA are compared, it is clear that the ISSA performs better in dampening oscillations and improves the dynamic stability of the power system. These graphs illustrate that the controllers created using the suggested way perform better and have more features than those created using other methods. Note that $w_{12} = w_2 - w_1$ and $w_{13} = w_3 - w_1$.

VII. CONCLUSION

The primary objective of the research is to develop an improved version of the salp swarm algorithm (ISSA). To strengthen the suggested ISSA's search and discovery capabilities, two additional equations for the leader and followers updating positions are introduced. In addition, the ISSA substitutes the worst salp giving the highest fitness value with a randomly generated salp at each generation. To obtain an appropriate assessment of the new algorithm's performance, a statistical study is performed. According to the findings of a comparison of the proposed algorithm on some well-known unimodal and multimodal test functions, the suggested technique performs significantly in terms of stability, accuracy and flexibility. The paper's second purpose is to create coordinated design controllers at the same time. To demonstrate the utility of the proposed ISSA in addressing real-world optimization issues, we employ the novel technique to develop UPFC controllers as a sophisticated

numerical optimization problem. When the ISSA and TSA findings are compared, it is obvious that the ISSA performs better and is more effective in dampening low frequency oscillation in multi-power systems. Several possible applications and research paths might be suggested for future study. The suggested technique may address a wide range of engineering issues, such as damping controller design, pipe routing design, optimal power flow problems, neural network training, and image processing. One of the constraints of the proposed ISSA, like other stochastic optimization approaches, is that new optimizers may be created in the future that achieve better than ISSA in some real-world situations. Furthermore, because the ISSA is stochastic, it cannot be guaranteed that the solutions derived using the ISSA are precisely equivalent to the global optimal for all optimization problems.

REFERENCES

[1] P. Kundur, N. J. Balu, and M. G. Lauby, *Power System Stability and Control* vol. 7. New York, NY, USA: McGraw-Hill, 1994.

[2] M. Eslami, H. Shareef, A. Mohamed, and M. Khajehzadeh, "A survey on flexible AC transmission systems (FACTS)," *Przeglad Elektrotechniczny*, vol. 88, no. 1, pp. 1–11, 2012.

[3] L. Gyugyi, C. D. Schauder, S. L. Williams, T. R. Rietman, D. R. Torgerson, and A. Edris, "The unified power flow controller: A new approach to power transmission control," *IEEE Trans. Power Del.*, vol. 10, no. 2, pp. 1085–1097, Apr. 1995.

[4] M. Eslami, H. Shareef, M. R. Taha, and M. Khajehzadeh, "Adaptive particle swarm optimization for simultaneous design of UPFC damping controllers," *Int. J. Electr. Power Energy Syst.*, vol. 57, pp. 116–128, May 2014.

[5] M. Eslami, H. Shareef, A. Mohamed, and M. Khajehzadeh, "Damping of power system oscillations using genetic algorithm and particle swarm optimization," *Int. Rev. Electr. Eng.*, vol. 5, no. 6, pp. 2745–2753, 2010.

[6] M. Eslami, H. Shareef, A. Mohamed, and M. Khajehzadeh, "Damping controller design for power system oscillations using hybrid GA-SQP," *Int. Rev. Electr. Eng.*, vol. 6, no. 2, pp. 888–896, 2011.

[7] M. Eslami, H. Shareef, and A. Mohamed, "Optimization and coordination of damping controls for optimal oscillations damping in multi-machine power system," *Int. Rev. Electr. Eng.*, vol. 6, no. 4, pp. 1984–1993, 2011.

[8] M. Eslami, H. Shareef, A. Mohamed, and M. Khajehzadeh, "Optimal location of PSS using improved PSO with chaotic sequence," in *Proc. Int. Conf. Electr., Control Comput. Eng. (InECCE)*, Jun. 2011, pp. 253–258.

[9] M. Eslami, H. Shareef, A. Mohamed, and M. Khajehzadeh, "Particle swarm optimization for simultaneous tuning of static VAR compensator and power system stabilizer," *Przegląd Elektrotechniczny*, vol. 87, pp. 343–347, Jan. 2011.

[10] M. Eslami, H. Shareef, A. Mohamed, and M. Khajehzadeh, "PSS and TCSC damping controller coordinated design using GSA," *Energy Proc.*, vol. 14, pp. 763–769, Jan. 2012.

[11] Y.-S. Chuang, C.-J. Wu, S.-C. Wang, and P.-H. Huang, "Pole placement design of decentralized output feedback power system stabilizers using hybrid differential evolution," *J. Mar. Sci. Technol.*, vol. 15, no. 4, pp. 339–350, Aug. 2007.

[12] M. Khajehzadeh, M. R. Taha, and M. Eslami, "Multi-objective optimization of foundation using global-local gravitational search algorithm," *Struct. Eng. Mech.*, vol. 50, no. 3, pp. 257–273, May 2014.

[13] M. A. Kamarposhti, I. Colak, C. Iwendi, S. S. Band, and E. Ibeke, "Optimal coordination of PSS and SSSC controllers in power system using ant colony optimization algorithm," *J. Circuits, Syst. Comput.*, vol. 31, no. 4, Mar. 2022, Art. no. 2250060.

[14] M. Eslami, H. Shareef, and M. Khajehzadeh, "Optimal design of damping controllers using a new hybrid artificial bee colony algorithm," *Int. J. Electr. Power Energy Syst.*, vol. 52, pp. 42–54, Nov. 2013.

[15] M. A. Abido and Y. L. Abdel-Magid, "Coordinated design of a PSS and an SVC-based controller to enhance power system stability," *Int. J. Electr. Power Energy Syst.*, vol. 25, no. 9, pp. 695–704, Nov. 2003.

[16] M. Eslami, M. Neshat, and S. A. Khalid, "A novel hybrid sine cosine algorithm and pattern search for optimal coordination of power system damping controllers," *Sustainability*, vol. 14, no. 1, p. 541, Jan. 2022.

[17] A. Noori, M. J. Shahbazadeh, and M. Eslami, "Designing of wide-area damping controller for stability improvement in a large-scale power system in presence of wind farms and SMES compensator," *Int. J. Electr. Power Energy Syst.*, vol. 119, Jul. 2020, Art. no. 105936.

[18] J. Bhukya, T. A. Naidu, S. Vuddanti, and C. Konstantinou, "Coordinated control and parameters optimization for PSS, POD and SVC to enhance the transient stability with the integration of DFIG based wind power systems," *Int. J. Emerg. Electr. Power Syst.*, vol. 23, no. 3, pp. 359–379, Jun. 2022.

[19] S. M. A. Elazim and E. S. Ali, "Optimal power system stabilizers design via Cuckoo search algorithm," *Int. J. Electr. Power Energy Syst.*, vol. 75, pp. 99–107, Feb. 2016.

[20] M. Eslami, B. Babaei, H. Shareef, M. Khajehzadeh, and B. Arandian, "Optimum design of damping controllers using modified sperm swarm optimization," *IEEE Access*, vol. 9, pp. 145592–145604, 2021.

[21] M. A. Abido and Y. L. Abdel-Magid, "A Tabu search based approach to power system stability enhancement via excitation and static phase shifter control," *Electr. Power Syst. Res.*, vol. 52, no. 2, pp. 133–143, Nov. 1999.

[22] M. A. Abido, "Simulated annealing based approach to PSS and FACTS based stabilizer tuning," *Int. J. Electr. Power Energy Syst.*, vol. 22, no. 4, pp. 247–258, May 2000.

[23] M. Khajehzadeh, M. R. Taha, and M. Eslami, "A new hybrid firefly algorithm for foundation optimization," *Nat. Acad. Sci. Lett.*, vol. 36, no. 3, pp. 279–288, Jun. 2013.

[24] M. Khajehzadeh, M. R. Taha, and M. Eslami, "Multi-objective optimisation of retaining walls using hybrid adaptive gravitational search algorithm," *Civil Eng. Environ. Syst.*, vol. 31, no. 3, pp. 229–242, Jul. 2014.

[25] S. Mirjalili, S. M. Mirjalili, and A. Hatamlou, "Multi-verse optimizer: A nature-inspired algorithm for global optimization," *Neural Comput. Appl.*, vol. 27, no. 2, pp. 495–513, 2016.

[26] S. Kaur, L. K. Awasthi, A. L. Sangal, and G. Dhiman, "Tunicate swarm algorithm: A new bio-inspired based metaheuristic paradigm for global optimization," *Eng. Appl. Artif. Intell.*, vol. 90, Apr. 2020, Art. no. 103541.

[27] S. Mirjalili, A. H. Gandomi, S. Z. Mirjalili, S. Saremi, H. Faris, and S. M. Mirjalili, "Salp swarm algorithm: A bio-inspired optimizer for engineering design problems," *Adv. Eng. Softw.*, vol. 114, pp. 163–191, Dec. 2017.

[28] S. Li and L. Wu, "An improved salp swarm algorithm for locating critical slip surface of slopes," *Arabian J. Geosci.*, vol. 14, no. 5, pp. 1–11, Mar. 2021.

[29] M. Khajehzadeh, S. Keawsawasvong, and M. L. Nehdi, "Effective hybrid soft computing approach for optimum design of shallow foundations," *Sustainability*, vol. 14, no. 3, p. 1847, Feb. 2022.

[30] H. F. Wang, "Applications of modelling UPFC into multi-machine power systems," *IEE Proc. Gener., Transmiss. Distrib.*, vol. 146, no. 3, pp. 306–312, May 1999.

[31] H. Wang, "A unified model for the analysis of FACTS devices in damping power system oscillations. III. Unified power flow controller," *IEEE Trans. Power Del.*, vol. 15, no. 3, pp. 978–983, Jul. 2000.

[32] K. Zervoudakis and S. Tsafarakis, "A mayfly optimization algorithm," *Comput. Ind. Eng.*, vol. 145, Jul. 2020, Art. no. 106559.

[33] J. Kennedy and R. Eberhart, "Particle swarm optimization," in *Proc. Int. Conf. Neural Netw.*, vol. 4. Perth, WA, Australia, Nov. 1995, pp. 1942–1948.

[34] X. S. Yang, "Firefly algorithms for multimodal optimization," in *Proc. Int. Symp. Stochastic Algorithms*, in Lecture Notes in Computer Sciences, vol. 5792, 2009, pp. 169–178.

[35] G. Dhiman, M. Garg, A. Nagar, V. Kumar, and M. Dehghani, "A novel algorithm for global optimization: Rat swarm optimizer," *J. Ambient Intell. Humanized Comput.*, vol. 12, no. 8, pp. 8457–8482, 2020.

[36] G. Rogers, *Power System Oscillations*. Norwell, MA, USA: Kluwer, 2000.

[37] M. Eslami, H. Shareef, A. Mohamed, and M. Khajehzadeh, "An efficient particle swarm optimization technique with chaotic sequence for optimal tuning and placement of PSS in power systems," *Int. J. Elect. Power Energy Syst.*, vol. 43, no. 1, pp. 1467–1478, 2012, doi: 10.1016/j.ijepes.2012.07.028.

[38] J. Chow and G. Rogers, "Power system toolbox: A set of coordinated M-files for use with MATLAB," Cherry Tree Sci. Softw., Toronto, ON, Canada, 1996.

EHSAN AKBARI was born in Borujerd, Iran, in 1987. He received the B.Sc. and M.Sc. degrees in power electrical engineering from the Mazandaran University of Science and Technology (MUST), Babol, Iran, in 2010 and 2014, respectively. He has published more than 125 papers in reputed journals and conferences. His research interests include power quality and distribution flexible AC transmission systems (DFACTS), application of power electronics in power systems, power electronics multilevel converters, smart grids, harmonics and reactive power control using hybrid filters, and renewable energy systems. He is a Contributing Reviewer of *AJEEE* journal.

MORTEZA MOLLAJAFARI received the B.S. degree in electrical engineering from the Electrical Engineering Department, K. N. Toosi University of Technology, in 2008, and the M.Sc. and Ph.D. degrees in electrical engineering from the Iran University of Science and Technology (IUST), in 2011 and 2017, respectively. He is currently an Assistant Professor with the Automotive Engineering Department, IUST. His research interests include parallel and distributed computing systems, especially cloud computing, developing scheduling algorithms, evolutionary algorithms, and autonomous vehicular systems.

HAMZA MOHAMMED RIDHA AL-KHAFAJI (Senior Member, IEEE) received the B.Sc. degree in electronic and communications engineering and the M.Sc. degree in modern communications engineering from Nahrain University, Baghdad, Iraq, in 2004 and 2007, respectively, and the Ph.D. degree in communication engineering from Universiti Malaysia Perlis, in 2014. He has five years working experience as a Senior BSS Engineer at Huawei Technologies and Omnnea Wireless Telecom, Iraq, from 2006 to 2010. After that, he completed one year postdoctoral research at Universiti Teknologi Malaysia. He has been a Lecturer at the Al-Mustaqbal University College, Iraq, since September 2015. He has published more than 50 articles. His research interests include next generation wireless networks, the Internet of Things, and optical fiber communication systems. He is continuous in bringing new ideas to scientific research, combating the limitations, and seeking the next big things. He is a Senior Member of IACSIT and IEU and a member of IEICE, ACM, IAENG, SDIWC, ICSES, IASED, APSIPA, and QEAAS Society. He has served as an academic editor and a reviewer in many international journals and conferences.

HUSSEIN ALKATTAN is currently pursuing the Ph.D. degree with the Department of System Programming, South Ural State University, Chelyabinsk, Russia. He works in remote sensing, environmental science, image processing, steganography, ciphering, and satellite data analysis.

MOSTAFA ABOTALEB is currently pursuing the Ph.D. degree in developing artificial intelligence and machine learning models with South Ural State University, Russia, (direction of physics and mathematics). He is also a Faculty Member with the Computer Science Department, South Ural State University. Then, he became a Researcher Engineer in advanced research with the Department of System Programming, University of South Ural. In 2021, he got a patent from the Russian Federation for developing a library for forecasting COVID-19 infection cases using R programming. He has many publications related to developing deep learning models and classical models to improve the forecast through minimizing the error of forecast. He is currently designs machine learning algorithms. The connected machine learning algorithms in the drone can perform some advanced tasks. His aim is to discover a learning procedure that is efficient at finding complex structures in large, high-dimensional datasets and to show that this is how the brain learns to see. In addition, he reviewed some research papers in mathematics and deep learning in the top 10% indexed in Scopus.

MAHDIYEH ESLAMI (Member, IEEE) received the B.Sc. degree from the Bahonar University of Kerman, Iran, in 2000, the M.Sc. degree from the Iran University of Science and Technology (IUST), Tehran, Iran, in 2004, and the Ph.D. degree from the National University of Malaysia (UKM), in 2012, all in electrical engineering. From 2012 to 2013, she was a Postdoctoral Research Fellow with the Power Research Group, National University of Malaysia (UKM). She is currently an Assistant Professor with the Department of Electrical Engineering, Islamic Azad University, Kerman Branch. Since her Ph.D. degree, she has published more than 80 articles in various fields related to power system. Her research interests include power system stability, application of AI techniques in power systems, power system dynamics, and FACTS devices.

SIVAPRAKASAM PALANI received the B.E. degree in industrial engineering, the M.E. degree in computer integrated manufacturing, and the Ph.D. degree in mechanical engineering from the College of Engineering Guindy, Anna University, Chennai, India, in 2005, 2008, and 2015, respectively. He is currently working as an Associate Professor with Addis Ababa Science and Technology University, Ethiopia. He has 14 years of teaching and research experience, including international teaching experience in Oman and Ethiopia. He has published papers in 35 international journals and 23 international/national conferences. His research interests include micro/nano manufacturing, machining, composite materials, surface engineering, and optimization techniques.